Electrochimica Acta 66 (2012) 188–192

Contents lists available at SciVerse ScienceDirect

Electrochimica Acta

journal homepage: www.elsevier.com/locate/electacta

Effective immobilization of $Ru(bpy)_3^{2+}$ by functional composite phosphomolybdic acid anion on an electrode surface for solid-state electrochemiluminescene to sensitive determination of NADH

Yali Li[a,b], Xiurong Yang[b,*], Fan Yang[b], Yingping Wang[a,d], Peihua Zheng[c], Xiaoxu Liu[c]

[a] Institute of Special Wild Economic Animals and Plants, Chinese Academy of Agriculture Sciences, Changchun, Jilin 130122, China
[b] State Key Laboratory of Electroanalytical Chemistry, Changchun Institute of Applied Chemistry, Chinese Academy of Sciences, Changchun, Jilin 130022, China
[c] Flight Training Base, Air Force Aviation University, Changchun, Jilin 130022, China
[d] Kangmei Pharmaceutical Co., Ltd., Ji'an, Jilin 134200, China

ARTICLE INFO

Article history:
Received 17 November 2011
Received in revised form 19 January 2012
Accepted 21 January 2012
Available online 1 February 2012

Keywords:
Electrocatalytic oxidation
Hybrid nanocomposites
NADH
Polyoxometalates
Self-assembly
Solid-state electrochemiluminescence

ABSTRACT

Phosphomolybdic acid anion ($[PMo_{12}O_{40}]^{3-}$) was used for the immobilization of ruthenium(II) tris(bipyridine) ($Ru(bpy)_3^{2+}$) on an electrode surface to yield a sensitive solid-state electrogenerated chemiluminescence (ECL) sensor. $[PMo_{12}O_{40}]^{3-}$ anion in the prepared sensor had catalytic ability to the NADH oxidation. The ECL signal of the $Ru(bpy)_3^{2+}/[PMo_{12}O_{40}]^{3-}$ film was about 3-fold enhancement than that for the $Ru(bpy)_3^{2+}$/Nafion film to NADH determination. The resulting ECL sensor exhibited a wide linear range from 2.5×10^{-7} to 5.0×10^{-3} M ($R = 0.99$) with the detection limit of 1.67×10^{-8} M (S/N = 3). In addition, it had good reproducibility and excellent long-term stability, and the relative average deviation was 0.77% of ECL intensity–time curve under continuous potential scanning for 21 cycles; after being used in two weeks, the sensor was able to keep over 90% activity toward 25 μM NADH. Fabrication of the ECL sensor by this method is simple and easy. Such superior properties will promote the application of polyoxometalates in fabricating sensors for using in electroanalytical and biochemical analysis.

1. Introduction

The determination of reduced β-dihydronicotinamide adenine dinucleotide (NADH) is very important in enzyme assays, due to its participation in the enzymatic catalysis of hundreds of dehydrogenases useful both in bioprocesses and analytical applications [1]. The electrogenerated chemiluminescence (ECL) determination of NADH has been paid considerable attention because of the inherent advantages of ECL such as low background signal, simple optical setup, and versatility [2–4]. Among various ECL reagents, ruthenium(II) tris(bipyridine) ($Ru(bpy)_3^{2+}$) is selected and studied most extensively because of its superior properties including excellent stability, high sensitivity and good efficiency in aqueous solution [5]. Compared with those solution-phase ECL procedures, the immobilization of $Ru(bpy)_3^{2+}$ on solid electrode surfaces can provide several advantages such as reducing the consumption of expensive reagents, enhancing the ECL signal, and simplifying experimental design [6–9]. Thus increasing attention has been paid to immobilize $Ru(bpy)_3^{2+}$ on the electrode surfaces [10–15]. Some of the above mentioned methods possess a fast response and good stability, but the synthesis process is quite complicated and arduous. Recently, Sun et al. have prepared a series of ion conductors from cations $Ru(bpy)_3^{2+}$ and anions such as $PtCl_6^{2-}$, $AuCl_6^{2-}$ or citric-capped Au nanoparticles (NPs) via a solution-based self-assembly strategy to use in ECL detection [16–18]. The methods proposed by Sun et al. are relatively simple and the generated sensors exhibit excellent ECL behaviors, but the expensive precursors of the hybrids limit their application.

Polyoxometalates (POMs) as typical inorganic metal oxide clusters are very versatile inorganic building blocks for the construction of functional thin films [19]. POMs are usually used as the anionic moiety to attract and bond multiply charged cations in self-assembled films [20–22]. On the other hand, functional multilayer films containing POMs have potential application in electrocatalytic and photoluminescent materials [23]. POMs have been extensively applied as electrocatalysts in the past few years. The POMs of the films can catalyze both the reduction of ClO_3^-, BrO_3^-, IO_3^-, and the oxidation of $C_2O_4^-$, adrenaline, and NADH [24–26]. Therefore, the films containing POMs have potential applications in fabricating electrochemical sensors and biosensors. Although the investigations on $Ru(bpy)_3^{2+}$ and POMs are extensive (the studies mainly focused on the properties of transition metal ions and

* Corresponding author. Tel.: +86 0431 85262056; fax: +86 0431 85689278.
E-mail address: xryang@ciac.jl.cn (X. Yang).

0013-4686/$ – see front matter © 2012 Elsevier Ltd. All rights reserved.
doi:10.1016/j.electacta.2012.01.087

electrochemistry) [27–29], few studies report the synthesis of $Ru(bpy)_3^{2+}$/POMs via self-assemble strategy by simple mixing method and their corresponding ECL properties.

In the present work, the inexpensive charged anionic moieties Keggin 12-molybdophosphoric acid $[PMo_{12}O_{40}]^{3-}$ [30] were used to attract and bond multiply cations tris(2,2′-bipyridyl)ruthenium(II) ($Ru(bpy)_3^{2+}$) $[Ru(bpy)_3]^{2+}/[PMo_{18}O_{40}]^{3-}$ hybrid by simple mixing method. The compositions and microstructures of $[Ru(bpy)_3]^{2+}/[PMo_{18}O_{40}]^{3-}$ hybrid complex were characterized by elemental analysis (EDS), spectroscopic techniques (UV–vis, FTIR) and field-emission scanning electron microscopy (FE-SEM). The electrochemical and ECL behaviors of the $[Ru(bpy)_3]^{2+}/[PMo_{18}O_{40}]^{3-}$ hybrid complex contained in the solid film of the nanocomposites formed on the electrode surface were studied and found to exhibit a diffusion-controlled voltammetric feature and excellent ECL behaviors. $[PMo_{18}O_{40}]^{3-}$ in the $[Ru(bpy)_3]^{2+}/[PMo_{18}O_{40}]^{3-}$ hybrid complex showed electrocatalytic activity toward NADH oxidation and the $Ru(bpy)_3^{2+}$-NADH ECL system, therefore holds potential application as new electrochemiluminescent materials in electroanalytical and biochemical analysis field.

2. Experimental

2.1. Reagents

$H_3PMo_{12}O_{40}$ was purchased from Fluka. $Ru(bpy)_3Cl_2{\cdot}6H_2O$ was obtained from Aldrich. NADH was from Shanghai Biochemical Technology Company. All other chemicals and reagents were of analytical grade and were used as received without further purification.

2.2. Instruments and characterizations

The field-emission scanning electron microscopy (FE-SEM) measurements were carried out on a PHILIPS XL-30 ESEM with an accelerating voltage of 20 kV. The silicon slides were used as substrates for the FE-SEM experiments. EDS was performed using an EDAX system. UV–vis absorption spectra were detected from a Cary 50 UV–vis spectrometer (Varian, USA). Fourier transform infrared (FTIR) spectra were recorded on a FTIR spectrometer (Nicolet 520, USA) using the KBr wafer technique. Electrochemical experiments were carried out with a CHI 832 (Shanghai, China). In our three-electrode system, the ITO or $Ru(bpy)_3^{2+}/[PMo_{12}O_{40}]^{3-}$/ITO electrodes were selected as working electrodes. Ag/AgCl (saturated KCl) electrode was chosen as a reference electrode, and a platinum foil was employed as a counter electrode. It was worthwhile mentioning that the bare or $[Ru(bpy)_3]^{2+}/[PMo_{18}O_{40}]^{3-}$ nanocomposite-modified ITO electrodes at different steps were carried out in the place of the reservoir with a fixed area as it ensures the same electrode area, and the effective area was confined by the punched round hole with a diameter of 3 mm. The ECL signals were recorded with an MPI-A chemiluminescence analyzer (Xi' an Remax Science & Technology Company, Xi' An, China). The photomultiplier tube was biased at 800 V.

2.3. $Ru(bpy)_3^{2+}$ nanocomposites containing $H_3PMo_{12}O_{40}$ preparation and sensors fabrication

In a typical experiment, 100 μL of 0.2 mM $H_3PMo_{12}O_{40}$ was diluted to 1 mL aqueous solution firstly, and then a certain volume of 0.03 mM $Ru(bpy)_3^{2+}$ aqueous solution was added into the resulting solution under vigorous stirring. Several minutes later, the formation of a large amount of brown precipitates occurred. The resulting precipitates were collected by centrifugation, washed several times with water, and finally suspended in water for the further experiments.

Sensors were fabricated by sonicating and rinsing ITO electrodes firstly, and then a 10 μL aliquot of as-prepared suspension was coated on the ITO electrode. Finally, a completely dry brown $Ru(bpy)_3^{2+}/[PMo_{12}O_{40}]^{3-}$ composite film modified ITO electrode was obtained.

3. Results and discussion

3.1. SEM characterization

Fig. 1A shows typical SEM of the resulting precipitates of sample $[Ru(bpy)_3]^{2+}/[PMo_{12}O_{40}]^{3-}$. It was clear that the precipitates consisted of a large quantity of spherical shaped nanocomposites in a relative uniform size range. Their chemical composition was determined by the EDS analysis. As shown in Fig. 1B, despite the Si and Au elements originated from the substrate, the peaks were indexed to Ru, P, Mo, C, O, and N elements. The atom number ratio of Ru and Mo in the as-formed nanocomposites was 9.89:74.76, which was consistent with the 3:2 reaction molar ratio of $Ru(bpy)_3^{2+}$ to $PMo_{12}O_{40}^{3-}$. Considering the positive charge of $Ru(bpy)_3^{2+}$ ions and the negative charge of $PMo_{12}O_{40}^{3-}$ groups, the electrostatic attractions between these two complexes may impulse these supramolecular composites formation, and the unique properties of POMs such as counter-ion, small size and very high electronic density may play an important role in the hybrids fabrication. Similar assumption was discussed in the previous report [31].

Inset of Fig. 1A shows an SEM image of the resulting aggregates coated on an ITO substrate, indicating that the aggregates form a fairly smooth film on the substrate. No cracks are observed in the film suggest the $H_3PMo_{12}O_{40}$ had good ability to form films [20–22].

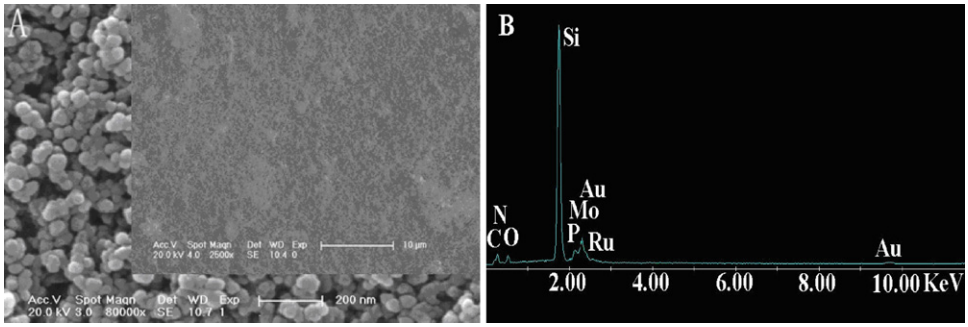

Fig. 1. (A) The FE-SEM image of the $[Ru(bpy)_3]^{2+}/[PMo_{12}O_{40}]^{3-}$ aggregates. (Inset of A) The $[Ru(bpy)_3]^{2+}/[PMo_{12}O_{40}]^{3-}$ aggregates formed on an ITO substrate and (B) the corresponding EDS of 1 mL 0.2 mM $PMo_{12}O_{40}^{3-}$ and 1 mL 0.03 mM $Ru(bpy)_3^{2+}$ formed aggregates.

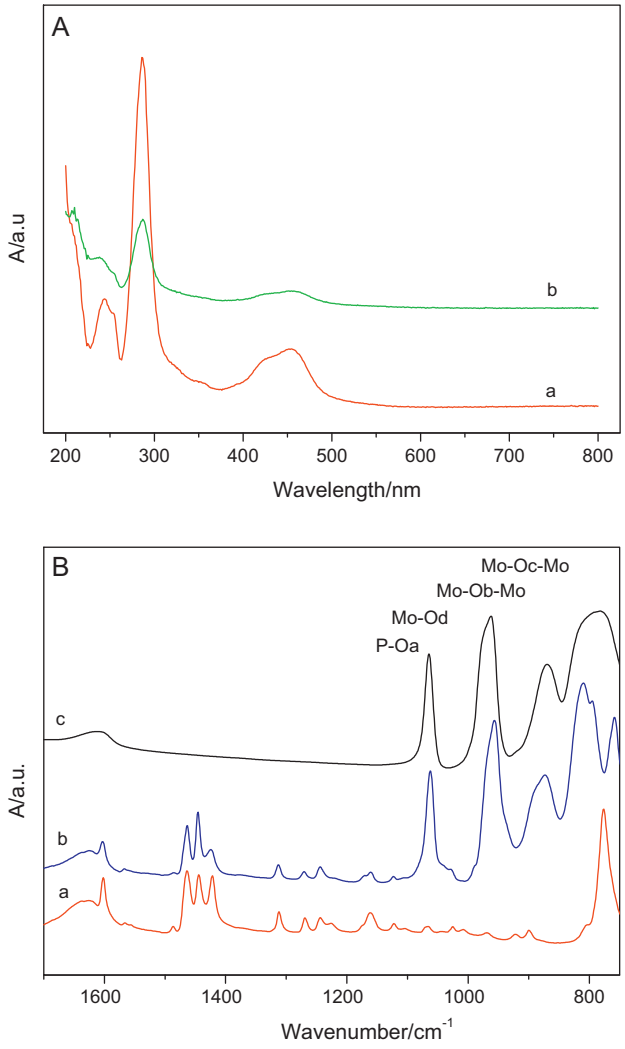

Fig. 2. (A) UV–vis absorbance spectra of free $Ru(bpy)_3Cl_2$ (curve a) and $[Ru(bpy)_3]^{2+}/[PMo_{12}O_{40}]^{3-}$ complex (curve b) in aqueous solution. (B) FTIR spectra of the free $Ru(bpy)_3^{2+}$ (curve a), $[Ru(bpy)_3]^{2+}/[PMo_{12}O_{40}]^{3-}$ complex (curve b) and pure $H_3PMo_{12}O_{40}$ (curve c).

3.2. Spectra study of the $[Ru(bpy)_3]^{2+}/[PMo_{12}O_{40}]^{3-}$ hybrid nanocomposites

The UV–vis absorption spectra of the $Ru(bpy)_3^{2+}$ aqueous solution and their hybrid complex were collected and compared. For free $Ru(bpy)_3Cl_2$ solution (Fig. 2A, curve a), two obvious peaks appeared at about 286.0 and 454.0 nm, which were assigned to ligand-centered transitions and metal-to-ligand charge transfer (MLCT), respectively [3]. For the $[Ru(bpy)_3]^{2+}/[PMo_{12}O_{40}]^{3-}$ hybrid complex (Fig. 2A, curve b), the similar absorption peaks were found except a little red-shift phenomenon. The little red shift for absorption peaks was further proving the strong electrostatic interaction between $Ru(bpy)_3^{2+}$ and negatively charged $[PMo_{12}O_{40}]^{3-}$ [3,5].

It was commonly seen that $[Ru(bpy)_3]Cl_2$ exhibited the typical FTIR peaks in the range 1400–1650 cm^{-1} (Fig. 2B, curve a), which are characteristic of 2,2′-bpy [32]. There were not change in the position of 2,2′-bpy moieties between 1400 and 1650 cm^{-1}, P—O bond at 1060 cm^{-1} and Mo=O terminal bond at 962 cm^{-1} in $[Ru(bpy)_3]^{2+}/[PMo_{12}O_{40}]^{3-}$ complex (Fig. 2B, curve b). However, the bands assigned to the edge Mo—O—Mo bond and to vertex Mo—O—Mo bond at 782 and 870 cm^{-1} in pure $H_3PMo_{12}O_{40}$ (Fig. 2B, curve c), appearing at higher wavenumbers in $[Ru(bpy)_3]^{2+}/[PMo_{12}O_{40}]^{3-}$ nanocomposites (Fig. 2B, curve b), 810 and 873 cm^{-1}, respectively. These frequency shifts were attributed to the interaction of $PMo_{12}O_{40}^{3-}$ with $Ru(bpy)_3^{2+}$, indicating an improved stability of $[PMo_{12}O_{40}]^{3-}$ inside the material [33–35]. These changes of spectra indicate that $Ru(bpy)_3^{2+}$ have been successfully immobilized in the hybrids via the electrostatic interaction using the simple mixing method.

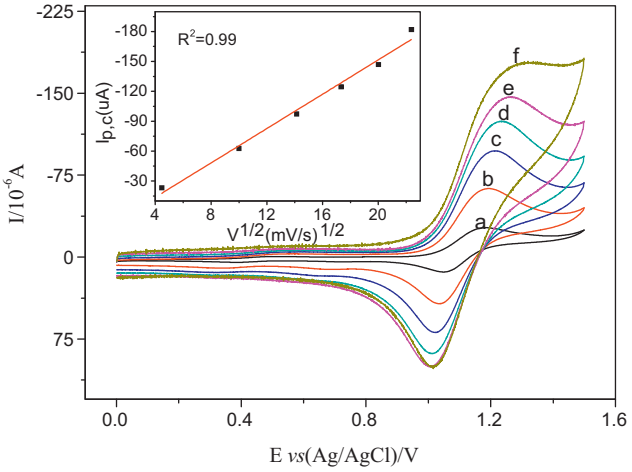

Fig. 3. Cyclic voltammetries of the nanocomposites $[Ru(bpy)_3]^{2+}/[PMo_{12}O_{40}]^{3-}$ coated on an ITO electrode in 100 mM phosphate buffer solution (PBS, pH 7.0) at different scan rates. Inset: the relationship between the anodic peak current and the square root of the scan rate $V^{1/2}$.

3.3. Electrochemistry and ECL investigation of the $[Ru(bpy)_3]^{2+}/[PMo_{12}O_{40}]^{3-}$ hybrid nanocomposites

Different cyclic voltammogram behaviors of as-prepared $Ru(bpy)_3^{2+}/[PMo_{12}O_{40}]^{3-}$ hybrids at different scan rates were investigated. As shown in Fig. 3, a pair of redox waves appeared at 1.18 V (vs Ag/AgCl), which was attributed to the one-electron redox reaction of $Ru(bpy)_3^{2+}$. The anodic peak current was proportional to the square root of scan rate $V^{1/2}$ in the range of 100–500 mV s^{-1} (as shown in curve b of inset of Fig. 3, $R^2 = 0.99$) indicating that the $Ru(bpy)_3^{2+}$ components contained in the nanocomposites on the electrode surface underwent a diffusion-controlled process within the film, which was similar to Sun et al. report [18]. It was clear that the peak separation increases with the increase of the scan rate, showing that the process was a quasi-reversible electrochemical process.

To study the ECL behaviors of $Ru(bpy)_3^{2+}/[PMo_{12}O_{40}]^{3-}$ hybrids, $Ru(bpy)_3^{2+}$/Nafion and $Ru(bpy)_3^{2+}/[PMo_{12}O_{40}]^{3-}$ hybrid coated ITO electrodes were both applied. For ensuring an equal quantity of $Ru(bpy)_3^{2+}$ in the films, an aliquot $Ru(bpy)_3^{2+}$ in the $Ru(bpy)_3^{2+}/[PMo_{12}O_{40}]^{3-}$ and $Ru(bpy)_3^{2+}$/Nafion was used to fabricate the films onto the ITO electrodes. In the present investigation, NADH was used as the ECL co-reactant. In the presence of the NADH, the ECL mechanisms of $Ru(bpy)_3^{2+}$ could be expressed as the following equations [36],

$$NADH \rightarrow NADH^{\bullet+} + e^- \quad (1)$$

$$Ru(bpy)_3^{2+} \rightarrow Ru(bpy)_3^{3+} + e^- \quad (2)$$

$$Ru(bpy)_3^{3+} + NADH \rightarrow Ru(bpy)_3^{2+} + NADH^{\bullet+} \quad (3)$$

$$NADH^{\bullet+} \rightarrow NAD^{\bullet} + H^+ \quad (4)$$

$$Ru(bpy)_3^{3+} + NAD^{\bullet} \rightarrow Ru(bpy)_3^{2+*} + NAD^+ \quad (5)$$

$$Ru(bpy)_3^{2+*} \rightarrow Ru(bpy)_3^{2+} + h\nu_{ECL} \quad (6)$$

For comparison, control experiments were done to investigate the ECL behaviors without and with the co-reactant NADH

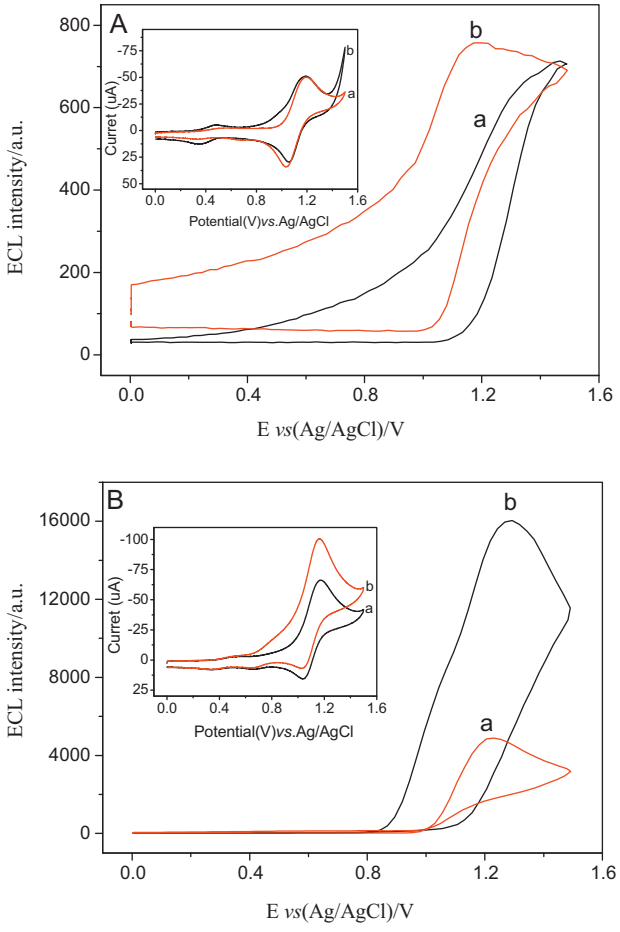

Fig. 4. ECL intensity–potential curve of $[Ru(bpy)_3]^{2+}$/Nafion/ITO electrode (curve a) and $[Ru(bpy)_3]^{2+}/[PMo_{12}O_{40}]^{3-}$/ITO electrode (curve b) in the absence of (A) and presence of (B) 100 μM NADH at a scan rate of 500 mV s^{-1}. Inset: the corresponding cyclic voltammetries at a scan rate of 100 mV s^{-1}.

employed different electrodes. Fig. 4A shows that the ECL signals had no obvious difference between $Ru(bpy)_3^{2+}$/Nafion and $Ru(bpy)_3^{2+}/[PMo_{12}O_{40}]^{3-}$ film without NADH. However, Fig. 4B indicates that the ECL signal of the $Ru(bpy)_3^{2+}/[PMo_{12}O_{40}]^{3-}$ film was about 3-fold enhancement than that observed for $Ru(bpy)_3^{2+}$/Nafion film to NADH determination.

In order to identify the function of $H_3PMo_{12}O_{40}$ in ECL processes, electrochemical behaviors of $Ru(bpy)_3^{2+}$/Nafion and $Ru(bpy)_3^{2+}/[PMo_{12}O_{40}]^{3-}$ composite-coated electrodes with and without NADH were studied. Cyclic voltammograms demonstrated that there was 1.5-fold enhancement in the presence of the NADH (inset of Fig. 4B) on the $Ru(bpy)_3^{2+}/[PMo_{12}O_{40}]^{3-}$ composite-coated electrodes, while the signals of current had no obvious difference in the absence of NADH on the above mentioned different electrodes (as shown in inset of Fig. 4A). These phenomena indicated that the presence of $PMo_{12}O_{40}^{3-}$ had catalytic ability to the NADH oxidation. So it can conclude that the presence of $H_3PMo_{12}O_{40}$ obviously decrease the potential barriers of Eq. (1). On the other hand, the large surface structure of the nanocomposite film (see the FE-SEM in Fig. 1) may facilitate the diffusion of NADH into the membrane and result in peak current and ECL signal enhancement occurring at the electrode interface.

The cyclic voltammograms for the electrocatalytic oxidation of NADH by $Ru(bpy)_3^{2+}/[PMo_{12}O_{40}]^{3-}$ film were investigated. With increasing the concentration of NADH, the anodic peak current of the E_{pa} value at about 1.18 V increased, and the corresponding of cathodic peak current decreased (data not shown here),

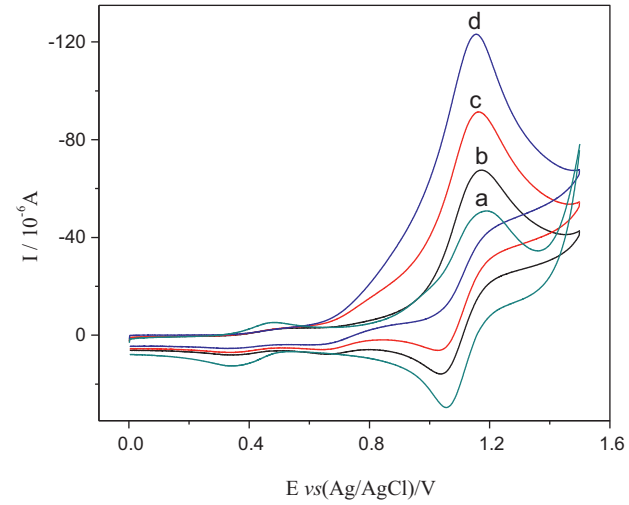

Fig. 5. Current intensity–potential curves (scan rate, 500 mV s^{-1}) of $[Ru(bpy)_3]^{2+}/[PMo_{12}O_{40}]^{3-}$ nanocomposite-coated ITO electrode containing NADH in various concentrations: 0, 50, 100 and 150 μM (curve a, b, c, and d) in 100 mM, pH 7.0 PBS respectively.

suggesting that the $Ru(bpy)_3^{2+}/[PMo_{12}O_{40}]^{3-}$ film showed electrocatalytic effect toward the oxidation of NADH due to the presence of $[PMo_{12}O_{40}]^{3-}$ in the films. It may be concluded that POMs served not only as the formed-film composites but also as an electrocatalyst. The corresponding ECL signals proportional to the concentration of NADH (as shown in Fig. 5) suggested the sensor can be used for NADH determination.

The calibration plot for NADH detection with the proposed biosensor was studied. The wide linear range covered from 2.5×10^{-7} to 5.0×10^{-3} M ($R = 0.99$) with the detection limit of 1.67×10^{-8} M (S/N = 3). Moreover, the stability of this biosensor was studied in different ways. There was no obvious change for ECL intensity under continuous potential scanning for 21 cycles in phosphate buffer solution (pH 7.0) containing 25 μM NADH as demonstrated in Fig. 6, and relative average deviation was 0.77%; the long-term stability of the biosensor was investigated during two weeks. The results suggested less than 10% decrease in ECL response to 25 μM NADH over this period. However, in previous report using the $[PW_{12}O_{40}]^{3-}$ to immobilize $Ru(bpy)_3^{2+}$, the

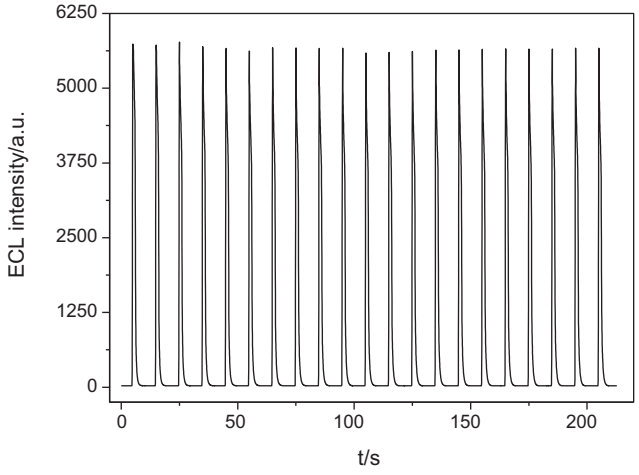

Fig. 6. ECL intensity–time curve of $[Ru(bpy)_3]^{2+}/[PMo_{12}O_{40}]^{3-}$ nanocomposite-coated ITO in the presence of 25 μM NADH under continuous cyclic voltammetry for 21 cycles in PBS pH 7.0 with the scan rate of 500 mV s^{-1}.

relative average deviation of the sensor under continuous potential scanning for 21 cycles was 4.38%, and the sensor lost 15% intensity compared to the initial [37]. The results indicated that the $[PMo_{12}O_{40}]^{3-}$ selected in this work hydrides with $Ru(bpy)_3^{2+}$ was more stable. The good stability and reproducibility can be explained as follows: first, $Ru(bpy)_3^{2+}$ is a very stable electrochemiluminescene reagent; second, the excellent film forming ability of the $PMo_{12}O_{40}^{3-}$ plays an important role in preventing the leakage of $Ru(bpy)_3^{2+}$. The results mentioned above would not only promote the development of novel ECL sensors based on $Ru(bpy)_3^{2+}$ doped with POMs, but also accelerate the use of POMs in analytical field.

4. Conclusion

In summary, the immobilization of $Ru(bpy)_3^{2+}$ by functional anion $[PMo_{12}O_{40}]^{3-}$ on an electrode surface provides an effective approach for the preparation of an enhanced ECL sensor. $[PMo_{12}O_{40}]^{3-}$ anion in the prepared sensor had catalytic ability to the NADH oxidation. The ECL signal of the $Ru(bpy)_3^{2+}/[PMo_{12}O_{40}]^{3-}$ film was about 3-fold enhancement than that at the $Ru(bpy)_3^{2+}$/Nafion film to NADH determination. Due to the good electronic conductivity and excellent electrocatalytic ability of $[PMo_{12}O_{40}]^{3-}$, the sensors show fast charge transfer and high sensitivity. This method is very simple, effective, and low cost, demonstrating the potential prospect of POMs in electroanalytical and bioanalytical fields.

Acknowledgments

This work was supported by the National Natural Science Foundation of China (No. 20890022) and the National Key Basic Research Development Project of China (No. 2010CB933602).

References

[1] M.J. Lobo, A.J. Miranda, P. Tunon, Amperometric biosensors based on NAD(P)-dependent dehydrogenase, Electroanalysis 9 (1997) 191.
[2] X.Q. Lin, F. Li, Y.Q. Pang, H. Cui, Flow injection analysis of gallic acid with inhibited electrochemiluminescence detection, Anal. Bioanal. Chem. 378 (2004) 2028.
[3] L. Qian, X.R. Yang, One-step synthesis of $[Ru(bpy)_3]^{2+}$ immobilized silica nanoparticles towards electrogenerated chemiluminescence detection, Adv. Funct. Mater. Adv. Funct. Mater. 17 (2007) 1353.
[4] R. Pyati, M. MarkRichter, ECL-electrochemical luminescence, Annu. Rep. Prog. Chem. C 103 (2007) 12.
[5] K. Honda, M. Yoshimura, T.N. Rao, A. Fujishima, Electrogenerated chemiluminescence of the ruthenium tris(2,2′-bipyridyl)/amines system on a boron-doped diamond electrode, J. Phys. Chem. B 107 (2003) 1653.
[6] H.S. White, A.J. Bard, Electrogenerated chemiluminescence and chemiluminescence of the $[Ru(bpy)_3]^{2+}$-$S_2O_8^{2-}$ system in acetonitrile–water solutions, J. Am. Chem. Soc. 104 (1982) 6891.
[7] T.A. Nieman, Modulated potential electrogenerated chemiluminescence of luminol and $Ru(bpy)_3^{2+}$, Microchim. Acta 113 (1994) 339.
[8] B.A. Gorman, P.S. Francis, N.W. Barnett, Tris(2,2′-bipyridyl)ruthenium(II) chemiluminescence, Analyst 131 (2006) 616.
[9] H. Wei, E.K. Wang, Solid-state electrochemiluminescence of tris(2,2′-bipyridyl) ruthenium, Trends Anal. Chem. 27 (2008) 447.
[10] A.N. Khramov, M.M. Collinson, Electrogenerated chemiluminescence of tris (2,2′-bipyridyl)ruthenium(II) ion-exchanged in nafion–silica composite films, Anal. Chem. 72 (2000) 2943.
[11] H.N. Choi, S.H. Cho, W.Y. Lee, Electrogenerated chemiluminescence from tris(2,2′-bipyridyl)ruthenium(II) immobilized in titania–perfluorosulfonated ionomer composite films, Anal. Chem. 75 (2003) 4250.
[12] J.K. Lee, S.H. Lee, M. Kim, H. Kim, D.H. Kim, W.Y. Lee, Organosilicate thin film containing $Ru(bpy)_3^{2+}$ for an electrogenerated chemiluminescence sensor, Chem. Commun. 13 (2003) 1602.
[13] G.M. Greenway, A. Greenwood, P. Watts, C. Wiles, Solid-supported chemiluminescence and electrogenerated chemiluminescence based on a tris(2,2′-bipyridyl)ruthenium(II) derivative, Chem. Commun. 1 (2006) 85.
[14] L. Armelao, R. Bertoncello, S. Gross, D. Badocco, P. Pastore, Construction and characterization of Ru(II)tris(bipyridine)-based silica thin film electrochemiluminescent sensors, Electroanalysis 15 (2003) 803.
[15] M.M. Collinson, B. Novak, S.A. Martin, J.S. Taussig, Electrochemiluminescence of ruthenium(II) tris(bipyridine) encapsulated in Sol–Gel glasses, Anal. Chem. 72 (2000) 2914.
[16] X.P. Sun, Y. Du, S.J. Dong, E.K. Wang, Method for effective immobilization of $[Ru(bpy)_3]^{2+}$ on an electrode surface for solid-state electrochemiluminescene detection, Anal. Chem. 77 (2005) 8166.
[17] X.P. Sun, Y. Du, L.H. Zhang, S.J. Dong, E.K. Wang, Pt nanoparticles: heat treatment-based preparation and $[Ru(bpy)_3]^{2+}$-mediated formation of aggregates that can form stable films on bare solid electrode surfaces for solid-state electrochemiluminescence detection, Anal. Chem. 78 (2006) 6674.
[18] X.P. Sun, Y. Du, L.H. Zhang, S.J. Dong, E.K. Wang, Luminescent supramolecular microstructures containing $[Ru(bpy)_3]^{2+}$: solution-based self-assembly preparation and solid-state electrochemiluminescence detection application, Anal. Chem. 79 (2007) 2588.
[19] C.L. Hill (Ed.), Introduction: polyoxometalates multicomponent molecular vehicles to probe fundamental issues and practical problems, Chem. Rev. 98 (1998) 1.
[20] N. Fay, E. Dempsey, T. McCrmac, Assembly, electrochemical characterisation and electrocatalytic ability of multilayer films based on $[Fe(bpy)_3]^{2+}$, and the Dawson heteropolyanion-$[P_2W_{18}O_{62}]^{6-}$, J. Electroanal. Chem. 574 (2005) 359.
[21] S.O. Liu, D.G. Kurth, H. Möhwald, D. Volkmer, A thin-film electrochromic device based on a polyoxometalate cluster, Adv. Mater. 14 (2002) 225.
[22] S.H. Gao, X. Li, C.P. Yang, T.H. Lia, R. Cao, Layer-by-Layer assembly of multilayer films of polyoxometalates and tris(phenanthrolinedione) complexes of transition metals, J. Solid State Chem. 179 (2006) 1407.
[23] K. Bineta, N. Louis, Polyoxometalate-based homogeneous catalysis of electrode reactions: recent achievements, J. Mol. Catal. A: Chem. 262 (2007) 190.
[24] E. Dempsey, A. Kennedy, N. Fay, T. McCormac, Investigations into heteropolyanions as electrocatalysts for the oxidation of adrenaline, Electroanalysis 15 (2003) 23.
[25] B. Keita, K. Essaadi, L. Nadjo, R. Contant, Y. Justum, Oxidation kinetics of NADH by heteropolyanions, J. Electroanal. Chem. 404 (1996) 271.
[26] H.Y. Ma, T. Dong, G. Wang, W. Zhang, F.P. Wang, X.D. Wang, Fabrication of self-assembled tris(1,10-phenanthroline)ruthenium/12-molybdophosphoric acid films with bifunctional electrocatalytic and photo-luminescent properties, Electroanalysis 18 (2006) 2475.
[27] A. Kuhn, F.C. Anson, Adsorption of monolayers of $P_2Mo_{18}O_{62}^{6-}$ and deposition of multiple layers of $Os(bpy)_3^{2+}$-$P_2Mo_{18}O_{62}^{6-}$ on electrode surfaces, Langmuir 12 (1996) 5481.
[28] V.M. Hultgren, A.M. Bond, A.G. Weld, Synthesis and electrochemistry of $[Ru(2,2'\text{-}bpy)_3]_2[S_2Mo_{18}O_{62}]$ at electrode–solvent (electrolyte) interfaces, J. Chem. Soc. Dalton Trans. (2001) 1076.
[29] L. Qian, X.R. Yang, Preparation and characterization of network composite film containing polyoxometalates and carbon nanotubes, Electrochem. Commun. 7 (2005) 547.
[30] B.R. Limogesa, R.J. Stanisa, J.A. Turnerb, A.M. Herringa, Electrochim. Acta 50 (2005) 1169.
[31] D. Ingersoll, P.J. Kulesza, L.R. Faulkner, Polyoxometalate-based layered composite films on electrodes-preparation through alternate immersions in modification solutions, J. Electrochem. Soc. 141 (1994) 140.
[32] Z. Han, E. Wang, G. Luan, Y. Li, C. Hu, P. Wang, N. Hu, H. Jia, Synthesis and crystal structure of a novel compound constructed from tris-(2,2′-bipy)ruthenium(II) and decatungstate, Inorg. Chem. Commun. 4 (2001) 427.
[33] J. Mosa, G. Larramona, A. Durán, M. Aparicio, Hydrophobic modification of poly(phthalazinone ether sulfone ketone) hollow fiber membrane for vacuum membrane distillation, J. Membr. Sci. 307 (2008) 21.
[34] M. Aparicio, J. Mosa, M. Etienne, A. Durán, Proton-conducting methacrylate-silica sol–gel membranes containing tungstophosphoric acid, J. Power Sources 145 (2005) 231.
[35] J.D. Kim, I. Honma, Proton conducting polydimethylsiloxane/zirconium oxide hybrid membranes added with phosphotungstic acid, Electrochim. Acta 48 (2003) 3633.
[36] C. Arnaud, G. Patrick, S. Neso, Bioelectrochemistry 69 (2006) 25.
[37] Y.L. Li, H. Zhu, X.R. Yang, $[Ru(bpy)_3]^{2+}$ nanocomposites containing heteropolyacids: simple preparation and stable solid-state electrochemiluminescence detection application, Talanta 80 (2009) 870.